

05,11

## Magnetization reorientation of GdFeCo/Ir/GdFeCo heterostructures at critical temperatures

© M.V. Bakhmetiev<sup>1</sup>, M.V. Burkanov<sup>2</sup>, R.A. Valeev<sup>2</sup>, V.P. Piskorskii<sup>2</sup>, R.B. Morgunov<sup>1,2,3</sup>

<sup>1</sup> Federal Research Center of Problems of Chemical Physics and Medicinal Chemistry RAS, Chernogolovka, Russia

<sup>2</sup> All-Russian Scientific Research Institute of Aviation Materials of the Research Center „Kurchatov Institute“, Moscow, Russia

<sup>3</sup> Tambov State Technical University, Tambov, Russia

E-mail: spintronics2022@yandex.ru

Received February 28, 2023

Revised February 28, 2023

Accepted March 1, 2023

In GdFeCo/Ir/GdFeCo heterostructures with amorphous GdFeCo layers, three critical points were found in the temperature dependences of the magnetization. In the neighborhood of 100 K, the temperature of compensation for the magnetizations of the Gd and FeCo sublattices is observed, which is found in the form of a magnetization minimum and does not depend on the magnetic field. As the temperature decreases, a sharp stepwise transition is observed, which corresponds to the switching of the mutual magnetization's orientation of the GdFeCo layers between their parallel and antiparallel configurations. This transition depends on the magnetic field in which the measurement is made. Its critical temperature shifts in the range of 70–300 K with a change in the field in the range of 0.5–5 T. At low temperatures < 50 K, a transition to the spin glass state is observed, which is accompanied by a decrease in the magnetic moment to zero and disappears when the field is applied.

**Keywords:** Compensation temperature, synthetic ferrimagnet, exchange interaction, magnetic anisotropy.

DOI: 10.21883/PSS.2023.05.56047.26

### 1. Introduction

Recently, GdFeCo thin films as part of various heterostructures have been extensively studied, because they exhibit a set of unusual effects associated with magnetization switching by polarized light (all-optical magnetization switching [1–3]) and with significant level of abnormal Hall effect in them [4–6]. It is commonly believed in literature that GdFeCo films are ferrimagnets both in crystalline and amorphous state [1–7]. Alloy of  $RE-TM$  and  $RE-TM-B$  ( $RE$  families — rare-earth metal,  $TM$  — transition metal,  $B$  — boron) in amorphous state can exhibit spin glass properties [8,9]. In  $RE-TM$  and  $RE-TM-B$  alloys, sublattice moment  $RE$  is associated with  $4f$ -electrons located much lower than the Fermi level, and sublattice moment  $TM$  corresponds to  $3d$ -electrons in whose energy zones the Fermi level is present. In [9], magnetic moments at deeper energy levels in TbCo alloy were found to change more easily by an external magnetic field than near the Fermi level while exhibiting characteristics similar to the spin glass such as slow dynamics and „freezing“ of magnetic moment.

Since the mentioned above investigations of the abnormal Hall effect and optical magnetization switching in GdFeCo are generally carried out at room temperature at which the use of heterostructure-based devices is expected, investigations of magnetization-temperature dependences of synthetic ferrimagnets - GdFeCo/Ir/GdFeCo, are carried out not so often. They are generally carried out to determine the

compensation point on monolayer samples. Compensation point in GdFeCo is important, because this is in its vicinity that the highest all-optical magnetization switching effect occurs. When discussing the obtained dependences of magnetization vs. temperature, the focus is made on the existence and position of the compensation point. Three spin-flip transitions observed on the temperature dependence of heterostructure magnetization are reported herein.

1. The compensation point characterizes the film material, depends on its chemical analysis and generally does not depend on the external magnetic field, because its position at the temperature scale is defined by the competition of sublattice exchange interaction energies. Sublattice exchange interaction energies are much higher than Zeeman interaction at any accessible laboratory magnetic fields.

2. Switching between mutual magnetizations of layers in the heterostructure is rather sensitive to the magnetic field and already in small magnetic fields, the temperature of such switching may be considerably changed by the magnetic field.

3. Transition between ferrimagnetic state of the alloy and spin glass state that is generally observed at low temperatures and is sensitive to external magnetic field.

Therefore, the purpose of the study was to separate the listed types of spin-flip transitions and to establish the temperature ranges and field where they are observed in GdFeCo/Ir/GdFeCo heterostructures.

## 2. Procedure and samples

$\text{Gd}_{0.25}[\text{Fe}_{0.9}\text{Co}_{0.1}]_{0.75}$  (5.2 nm)/Ir (0.6 nm)/  
 $\text{Gd}_{0.25}[\text{Fe}_{0.9}\text{Co}_{0.1}]_{0.75}$  (4.2 nm)/Cu (5.6 nm)/Ta (5 nm) multi-layer heterostructure was obtained by magnetron sputtering on Si/SiO<sub>2</sub> substrate with thermally grown 100 nm oxide layer to ensure insulation and prevent electric current leakage. After cutting and drying of samples in N<sub>2</sub> flow, the substrates were etched before each sputtering by 50 W high frequency Ar plasma at  $1 \cdot 10^{-2}$  mbar during 5 min. To obtain as uniform thin films as possible, the sample holder is rotated with a speed of  $\sim 10\text{--}30$  rpm. A Ta seed layer was sprayed before the magnetic layers of the structure in order to buffer substrate defects and facilitate the formation of Cu (111) texture favourable for formation of amorphous GdFeCo layer. Pt layer is added above as a protective layer. Perpendicular magnetic anisotropy is additionally improved when a GdFeCo layer is surrounded by Cu layers. When Gd content is within 20.2–25.9%, FeCo sublattice makes the dominating contribution to magnetization at room temperature.

Magnetic moment was measured using Quantum Design MPMS 5XL SQUID magnetometer in a constant field from  $-2$  to  $+2$  T at temperatures from 2 to 350 K.

The sample cross-section image was obtained using JEOL high resolution transmission electron microscope (HR TEM) at accelerating voltage 200 kV.

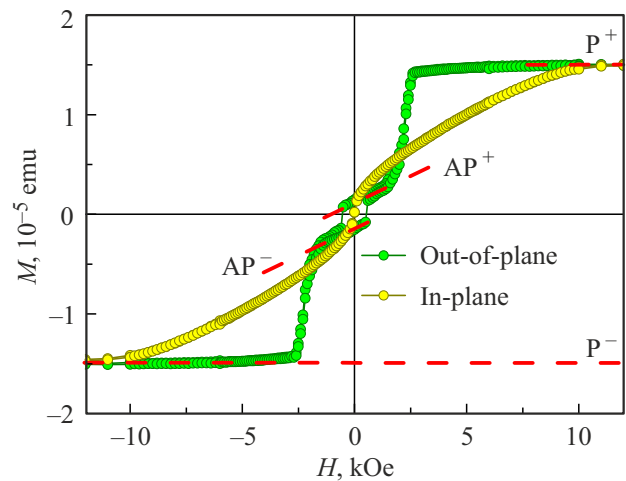
## 3. Experimental findings

Figure 1 shows magnetic hysteresis loops of GdFeCo/Ir/GdFeCo heterostructure measured at  $T = 300$  K in two magnetic field orientations with respect to the film plane when the field is in the sample plane (in-plane) and when the field is perpendicular to the sample plane (out-of-plane). Slow magnetization saturation with in-plane orientation indicates that magnetization in such orientation is described by a „hard plane“ model, and fast saturation in the field perpendicular to the sample indicates that this orientation coincides with the „easy axis“. In the easy axis orientation, four stable magnetization states P<sup>-</sup>, AP<sup>-</sup>, AP<sup>+</sup>, P<sup>+</sup> meeting the parallel and antiparallel mutual magnetization orientations of GdFeCo layers.

A set of magnetization hysteresis loops  $M(H)$  measured in the temperature range 2–350 K and field range from  $-2$  to  $+2$  T perpendicular to the sample plane is shown in Figure 2. It is shown that saturation magnetization at 2 T varies considerably and demonstrates its minimum near 100 K. Switching between states P<sup>-</sup>, AP<sup>-</sup>, AP<sup>+</sup>, P<sup>+</sup> is observed above 50 K and is absent at lower temperatures.

Figure 3 shows hysteresis loops in heterostructure plane field orientation. In this orientation, no transitions between states P<sup>-</sup>, AP<sup>-</sup>, AP<sup>+</sup>, P<sup>+</sup> are observed, however, the saturation magnetization minimum at 2 T occurs at 90–100 K.

Temperature dependences of saturation magnetization  $M_S$  are recorded in a strong magnetic field 2 T (Fig-

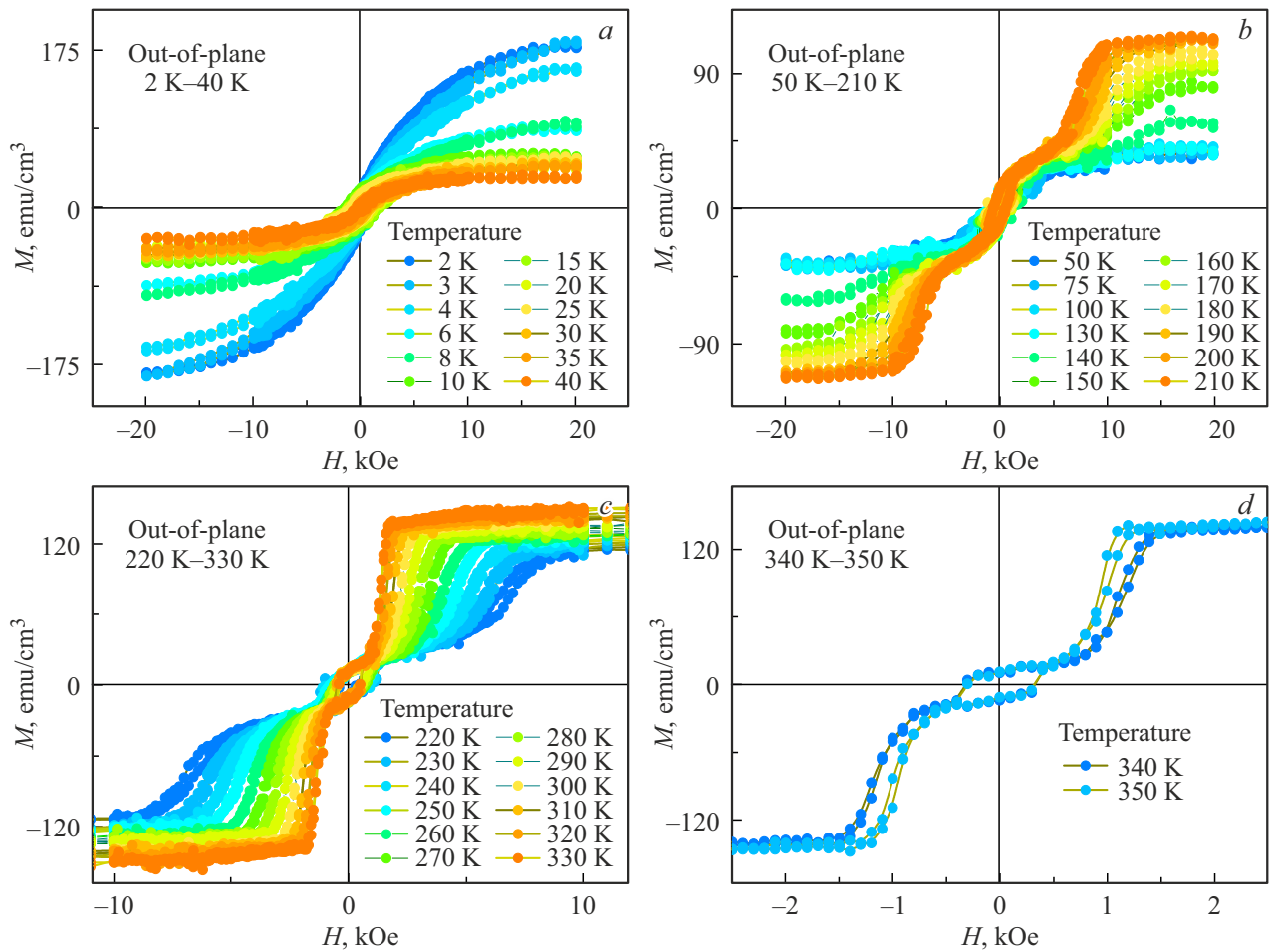


**Figure 1.** Magnetic hysteresis loops of GdFeCo/Ir/GdFeCo heterostructure measured at  $T = 300$  K in two magnetic field orientations with respect to the film plane, in-plane and out-of-plane. Dotted lines show P<sup>-</sup>, AP<sup>-</sup>, AP<sup>+</sup>, P<sup>+</sup> states meeting the parallel and antiparallel mutual magnetization orientations of GdFeCo layers.

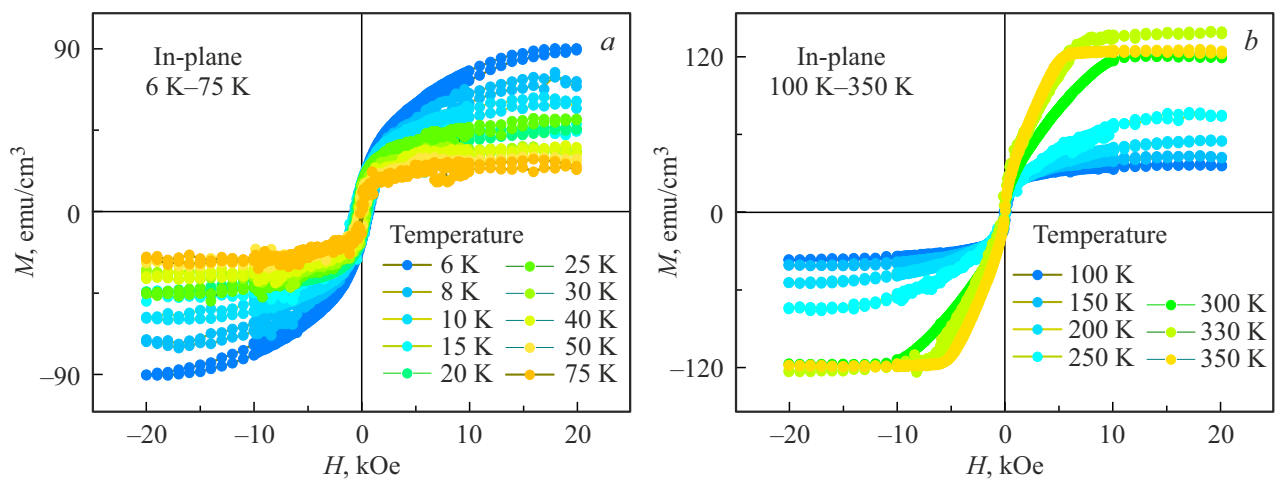
ure 4). Each point of the dependence corresponds to the hysteresis loop measured at this temperature. Magnetic moment  $M$  is normalized to Bohr magneton per  $\text{Gd}_{0.25}[\text{Fe}_{0.9}\text{Co}_{0.1}]_{0.75}$  formula unit. Saturation magnetization decreases within 2–50 K and grows at  $T = 70\text{--}350$  K (Figure 4). Flatness of curve  $M_S(T)$  at minimum values hinders the accurate measurement of compensation temperature. Difference between curves  $M_S(T)$  with in-plane and out-of-plane orientations occurs above 120 K, because the in-plane orientation corresponding to strong magnetization axis has a significant demagnetization field that reduces  $M_S$  (Figure 4). Dominance of Gd sublattice at low temperatures  $< 70$  K and dominance of CoFe sublattice at high temperatures  $> 100$  K can be suggested.

Figure 5 shows dependences of heterostructure magnetization vs. temperature measured with sample heating from 6 K at different magnetic field strengths perpendicular to the sample plane. It is shown that the magnetization minimum near 100 K (Figure 5, *d*) is overlapped by a sharp step-type transition when the magnetization grows by a factor of 5 near room temperature (Figure 5, *b*). Increase in the measurement magnetic field results in shift of this threshold transition towards low temperatures. Dependence of transition temperature  $T_{CR}$  vs. magnetic field  $H$  is shown in Figure 6.

In strong fields (Figure 5, *d*), a step-type transition is almost completely suppressed. And the compensation temperature becomes clearly visible, however, it does not result in zero magnetization. This may be explained by presence of two phases with different magnetic properties in films. Crystalline inclusions may have ferrimagnetic properties and demonstrate the compensation point. The



**Figure 2.** magnetization hysteresis loops measured at different temperatures in a magnetic field perpendicular to the sample plane.



**Figure 3.** Magnetization hysteresis loops measured at different temperatures in a magnetic field in the sample plane.

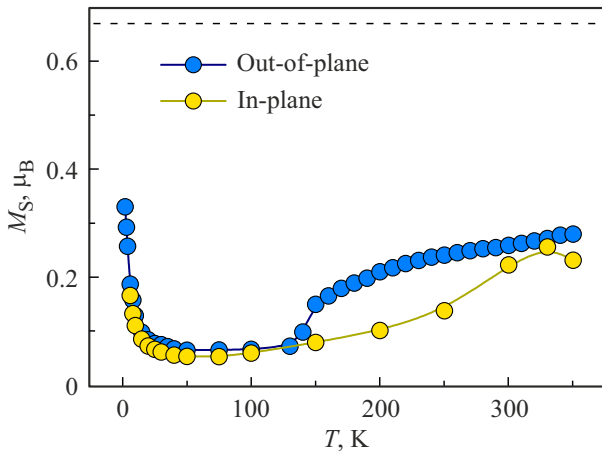


**Figure 4.** Temperature dependences of saturation magnetization measured in two field orientations: in/perpendicular to the film plane. Film magnetization was normalized to Bohr magneton and calculated for  $Gd_{0.25}[Fe_{0.9}Co_{0.1}]_{0.75}$  formula unit. Dashed line shows design value  $M_S$  calculated taking into account the sample stoichiometry, and magnetic moments of Gd, Fe and Co ions measured in [10,11] by X-ray magnetic chiral dichroism (XMCD).

co-existing amorphous phase may be in the spin glass state. In this case, when the compensation point is achieved in the ferrimagnetic part of the film, the spin glass magnetization will not be equal to zero as is shown by our experiments (Figure 5, *d*).

The crystalline region contribution hypothesis is supported by the sample cross-section image made by the transmission electron microscope (Figure 7). Near the interface in GdFeCo layer, extended crystalline inclusions with lattice constant corresponding to FeCo can be seen.

Figure 5, *b* shows the drop of the sample magnetic moment to zero in weak field 400 Oe in the temperature range below 50 K. This drop becomes weaker with field growth, and then in stronger fields up to 2 T, the magnetic field growth is observed. This is the third transition not caused by mutual layer magnetization switching and compensation point. Since this transition in a near-zero magnetic field results in disappearance of the sample magnetic field, this transition may be expected to be a transition to the spin glass state. This is proved by dependence of this transition on the magnetic field.

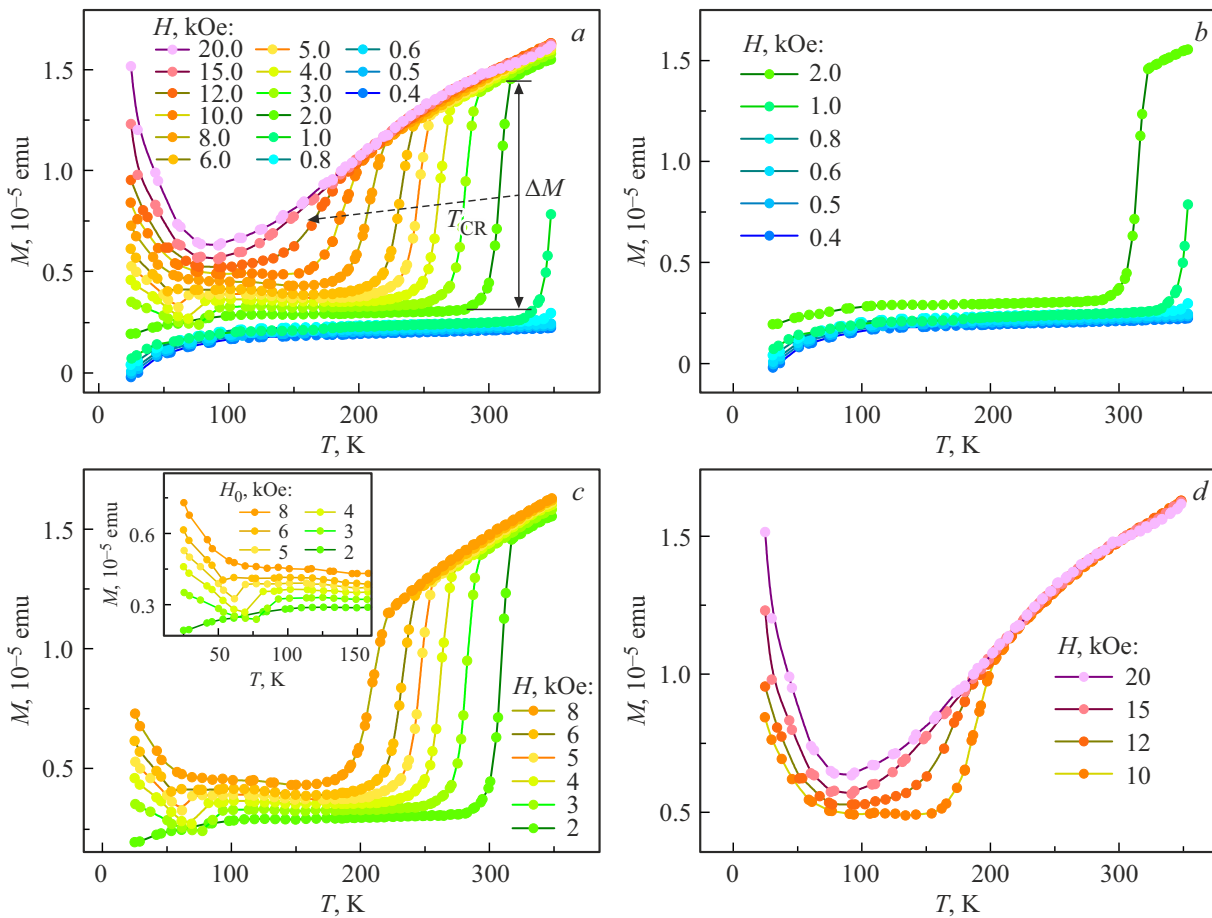


**Figure 5.** Temperature dependences of magnetic moment of GdFeCo film measures with sample heating after cooling in a zero field. The magnetic field is perpendicular to the film plane. diamagnetic contribution of the substrate was subtracted. The magnetic field applied during heating is shown on the curves: *a* — full dataset, *b* — field from 0.4 to 2.0 kOe, *c* — field from 2.0 to 8.0 kOe, *d* — field from 10.0 to 20.0 kOe.

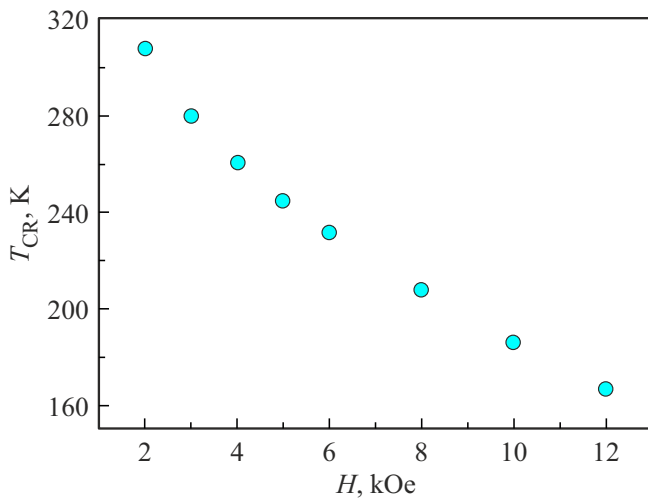


**Figure 6.** Dependence of transition temperature  $T_{CR}$  vs. magnetic field  $H$ .

#### 4. Discussion of experimental results

At 300 K, saturation magnetization  $M_S = 132 \text{ emu/cm}^3$  calculated at GdFeCo layer volume  $V_{\text{GdFeCo}} = 1.13 \cdot 10^{-7} \text{ cm}^3$  is in good agreement with the data in [12] for GdFeCo/Ir/GdFeCo heterostructure of the ferromagnetic layer with the same composition and the same thickness. Assuming the density of  $\text{Gd}_{0.24}\text{Fe}_{0.76}$  equal to  $\rho_{\text{GdFe}} = 7.87 \text{ g/cm}^3$  [13] and knowing the heterostructure dimensions (length  $a = 3 \text{ mm}$ , width  $b = 4 \text{ mm}$ ) and GdFeCo layer thickness ( $t_{\text{GdFeCo}} = 5.2 \text{ nm}$  for the upper layer and  $t_{\text{GdFeCo}} = 4.2 \text{ nm}$  for the lower layer), weight

$m_{\text{GdFeCo}}$  is calculated as follows:

$$\begin{aligned} m_{\text{GdFeCo}} &= \rho V = 7.87 \text{ g/cm}^3 \cdot 1.13 \cdot 10^{-7} \text{ cm}^3 \\ &= 8.89 \cdot 10^{-7} \text{ g.} \end{aligned}$$

Atomic weight of the formula unit is equal to

$$\begin{aligned} M_{\text{GdFeCo}} &= (0.25 M_{\text{Gd}} + 0.75(0.9 M_{\text{Fe}} + 0.1 M_{\text{Co}})) \\ &= (0.25 \cdot 157 + 0.75(0.9 \cdot 56 + 0.1 \cdot 59)) = 81.47, \end{aligned}$$

and corresponds to weight  $1.35 \cdot 10^{-22} \text{ g}$ .

The number of formula units in the film

$$N = \frac{m_{\text{GdFeCo}}}{M_{\text{GdFeCo}}} = \frac{8.89 \cdot 10^{-7} \text{ g}}{1.35 \cdot 10^{-22} \text{ g}} = 6.59 \cdot 10^{15}.$$

Saturation magnetization per formula unit at room temperature expressed in Bohr magnetons is:

$$\begin{aligned} \mu_{\text{GdFeCo}} &= \frac{M_S}{N} = \frac{1.63 \cdot 10^{-5} \text{ emu}}{6.59 \cdot 10^{15}} \\ &= 2.47 \cdot 10^{-21} \text{ emu} = 0.27 \mu_B. \end{aligned}$$

In [10,11], magnetic moments  $\text{Fe}^{2+}$ ,  $\text{Co}^{2+}$  and  $\text{Gd}^{3+}$  were found. We have used magnetic field strengths of  $\mu_{\text{FeCo}} = 1.3 \mu_B$  and  $\mu_{\text{Gd}} = 1.2 \mu_B$  obtained by XMCD method in films with similar composition to calculate the expected saturation magnetization in our  $\text{Gd}_{0.25}\text{Fe}_{0.675}\text{Co}_{0.075}$  sample. Appropriate atomic contributions per formula unit  $\mu_{\text{GdFeCo}} = 0.68 \mu_B$ . The fact that design value  $\mu_{\text{GdFeCo}}$  exceeds experimental value  $0.4 \mu_B$  may be explained by the amorphous structure of our samples. The calculations correspond to pure ferromagnetic state with parallel mutual

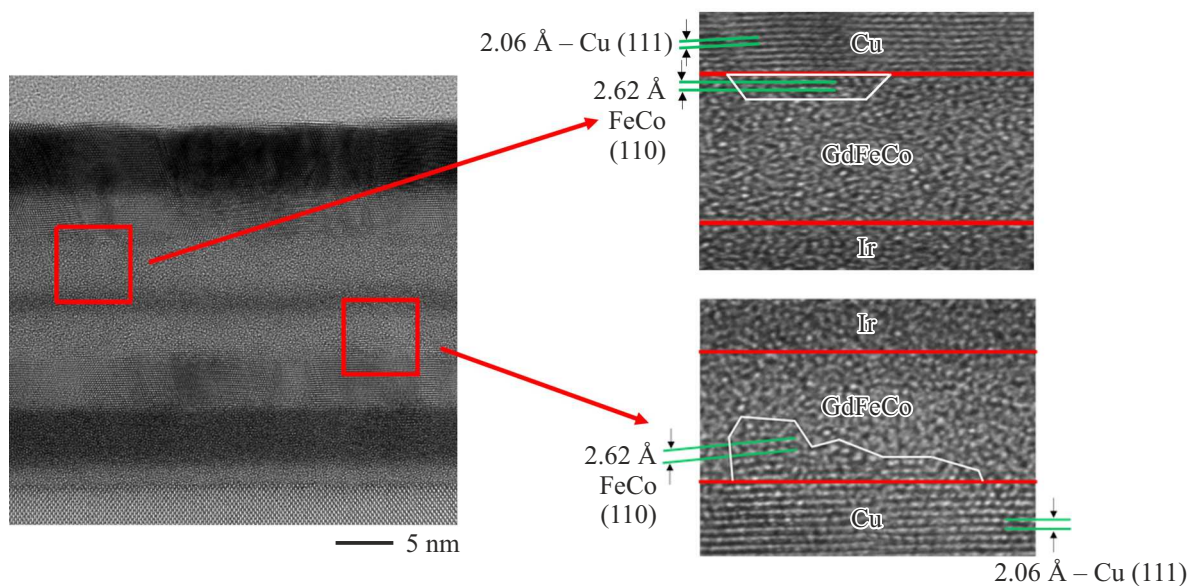


**Figure 7.** Sample cross-section image made by the transmission electron microscope (a). Zoomed in details of the heterostructure cross-section near GdFeCo/Cu interface (b).

orientation of spins, while the real sample is in amorphous state, where the spin glass and other noncollinear spin phases may contribute significantly to the total magnetization decreasing the final magnetization level.

Literature clearly illustrates the contribution of nonmagnetic layers to interlayer interaction due to the proximity effect. Additional magnetization appears in initially non-ferromagnetic heavy transition metals ( $TM = \text{Ir, Pt, etc.}$ ) bordering with the ferromagnet. Penetration of spin polarization into these metals from GdFeCo layer causes a so called magnetic proximity effect, i.e. spin polarization of metals  $TM$  at interfaces. For example, polarization Ir near Co/Ir boundary is equal to  $0.3\mu_B$  in [14]. Polarization of copper  $d$ -zone in multilayer Co/Cu structures is  $\sim 0.05\mu_B$  [15,16], and in multilayer Fe/Cu structures is  $\sim 0.09\mu_B$  [15]. These values are close to spin polarization of copper  $0.13\mu_B$  in FeCu and CoCu alloys [15–17] that could be formed as a result of copper diffusion into GdFeCo ferromagnetic layer. If the magnetizations of such phases make negative contributions to magnetization at room temperature, like  $\text{Gd}^{3+}$ , the resulting magnetization will be lower than its design value. When polarization of Fe ions is assumed equal to  $\mu_{\text{Fe}} = 0.2\mu_B$  [18] instead of  $\mu_{\text{FeCo}} = 1.3\mu_B$  in [10,11],  $\mu_{\text{GdFeCo}} = 0.15\mu_B$  will be obtained. Thus, experimental value  $M_S$  close to the assessments reported in literature may be also obtained taking into account the magnetization effects of transition metals.

Re-orientation sequence of ferrimagnetic layers depend on the ratio of exchange interaction and remagnetization barrier of ferrimagnetic layers [19]. Full energy  $E$  of two-layer GdFeCo sample is calculated using the equation describing the mutual magnetic moment orientation of two GdFeCo layers ( $M_1$  and  $M_2$ ):

$$E = E_Z + E_{\text{eff1}} + E_{\text{eff2}} + E_{EX}, \quad (1)$$

where  $E_Z$  is the Zeeman energy,  $E_{\text{eff1}}$  and  $E_{\text{eff2}}$  are the remagnetization energy barriers of upper and lower GdFeCo layers,  $E_{EX}$  is the exchange interaction energy between layers. All terms of equation (1) depend on the temperature and may be written as

$$E = H(M_1(T) + M_2(T)) + K_{\text{eff1}}(T) + K_{\text{eff2}}(T) - \frac{SJ(T)(M_1 + M_2)}{|M_1| \cdot |M_2|}, \quad (2)$$

where  $H$  is the external magnetic field,  $K_{\text{eff1}}$  and  $K_{\text{eff2}}$  are efficient anisotropy constants of GdFeCo layers,  $S$  is the interfacial area,  $J$  is the interlayer exchange interaction. Since  $K_{\text{eff1}}(T)$ ,  $K_{\text{eff2}}(T)$  and  $J(T)$  have various temperature dependences, energy balance is violated in favor of transition from  $P^+$  state to  $AP^+$  state.

## 5. Conclusions

1. It has been found that the saturation magnetization in GdFeCo/Ir/GdFeCo heterostructures differs from the

predicted simple ferrimagnetic model where magnetizations of Gd and FeCo sublattices are collinear and opposed to each other. It has been shown that, to explain the saturation field strengths, exchange interactions between sublattices shall be taken into account, because they result in incomplete compensation of magnetic moments of Gd and FeCo. Moreover, additional factors may appear such as iron and cobalt phases with diffusing copper and effects of transition metals proximity to a ferromagnet.

2. It has been found that the saturation magnetization dependence on temperature features the magnetization minimum whose position 90–100 K is independent of the applied field. This minimum corresponds to the compensation point of sublattices in the ferrimagnetic part of films.

3. The second sharp step-type transition is observed at 70–350 K. magnetization with temperature increase grows by a factor of five, position of this transition depends heavily on the magnetic field where measurements are carried out. This transition corresponds to switching of mutual orientation of magnetizations of two GdFeCo layers induced by the temperature and attributed to the change in the balance of anisotropy and antiferromagnetic exchange interaction constants between the layers. These characteristics grow with temperature decrease at various rates and ensure heterostructure switching to other stable state at lower temperature in the same field as at high temperature.

4. At low temperatures  $< 50$  K, the third transition is observed which is represented in the form of reduction of the sample magnetic moment to zero with temperature decrease. Application of the magnetic field removes this effect. It may be suggested that this transition is associated with the occurrence of the spin glass in the amorphous part of GdFeCo layer. Increased field leads to reduction of critical transition temperature to spin glass state and transforms the spin configuration from a disordered state to ferrimagnetic state.

## Acknowledgments

The authors are grateful to A.M. Kalashnikova for recommendations during preparation of this paper and to prof. Stephane Mangin for the samples provided for the study.

## Funding

The study was carried out as part of the thematic map of the Federal Research Center for Problems of Chemical Physics and Medical Chemistry of the RAS AAAA-A19-119111390022-2.

## Conflict of interest

The authors declare that they have no conflict of interest.



## References

- [1] L. Guyader, M. Savoini, S. Moussaoui, M. Buzzi, A. Tsukamoto, A. Itoh, A. Kirilyuk, T. Rasing, A.V. Kimel, F. Nolting. *Nature Commun.* **6**, 5839 (2015).
- [2] S. Iihama, Y. Xu, M. Deb, G. Malinowski, M. Hehn, J. Gorchon, E.E. Fullerton, S. Mangin. *Adv. Mater.* **30**, 1804004 (2018).
- [3] M.S. Hadri, P. Pirro, C.-H. Lambert, S. Petit-Watelot, Y. Quesab, M. Hehn, F. Montaigne, G. Malinowski, S. Mangin. *Phys. Rev. B* **94**, 064412 (2016).
- [4] Y. Wang, C. Li, H. Zhou, J. Wang, G. Chai, C. Jiang. *Appl. Phys. Lett.* **118**, 071902 (2021).
- [5] N. Roschewsky, T. Matsumura, S. Cheema, F. Hellman, T. Kato, S. Iwata, S. Salahuddin. *Appl. Phys. Lett.* **109**, 112403 (2016).
- [6] N. Roschewsky, C.-H. Lambert, S. Salahuddin. *Phys. Rev. B* **96**, 064406 (2017).
- [7] K. Wang, Y. Tang, K. Zhang, Y. Wang, J. Liu. *Mater. Sci. Eng. B* **263**, 114848 (2021).
- [8] J.F. Dillon. *J. Magn. Magn. Mater.* **31–34**, 1 (1983).
- [9] J.-H. Park, W.T. Kim, W. Won, J.-H. Kang, S. Lee, B.-G. Park, B.S. Ham, Y. Jo, F. Rotermund, K.-J. Kim. *Nature Commun.* **13**, 5530 (2022).
- [10] J. Sim, J.-H. Lee, S.-K. Kim. *J. Magn. Magn. Mater.* **542**, 168583 (2022).
- [11] T.A. Ostler, R.F.L. Evans, R.W. Chantrell, U. Atxitia, O. Chubykalo-Fesenko, I. Radu, R. Abrudan, F. Radu, A. Tsukamoto, A. Itoh, A. Kirilyuk, T. Rasing, A. Kimel. *Phys. Rev. B* **84**, 024407 (2011).
- [12] J.H. Kim, D.J. Lee, K.-J. Lee, B.-K. Ju, H.C. Koo, B.-C. Min, O.J. Lee. *Sci. Rep.* **8**, 6017 (2018).
- [13] R. Chimata, L. Isaeva, K. Kadas, A. Bergman, B. Sanyal, J.H. Mentink, M.I. Katsnelson, T. Rasing, A. Kirilyuk, A. Kimel, O. Eriksson, M. Pereiro. *Phys. Rev. B* **92**, 094411 (2015).
- [14] M. Perini, S. Meyer, B. Dupé, S. Malottki, A. Kubetzka, K. Bergmann, R. Wiesendanger, S. Heinze. *Phys. Rev. B* **97**, 184425 (2018).
- [15] G.A. Held, M.G. Samant, J. Stöhr, B. Hermsmeier, M. Schilfgaarde, R. Nakajimas. *Z. Phys. B* **100**, 335 (1997).
- [16] M.G. Samant, J. Stöhr, S.S.P. Parkin, G.A. Held, B.D. Hermsmeier, F. Herman, M.V. Schilfgaarde, L.-C. Duda, D.C. Mancini, N. Wassdahl, R. Nakajima. *Phys. Rev. Lett.* **72**, 1112 (1994).
- [17] W. Kuch, M. Salvietti, X. Gao, M. Klaua, J. Barthel, C.V. Mohan, J. Kirschner. *J. Appl. Phys.* **83**, 7019 (1998).
- [18] F. Wilhelm, P. Pouloupoulos, H. Wende, A. Scherz, K. Baberschke, M. Angelakeris, N.K. Flevaris, A. Rogalev. *Phys. Rev. Lett.* **87**, 207202 (2001).
- [19] O. Koplak, A. Talantsev, Y. Lu, A. Hamadeh, P. Pirro, T. Hauet, R. Morgunov, S. Mangin. *J. Magn. Magn. Mater.* **433**, 91 (2017).

*Translated by E.Ilyinskaya*